Evaluation of Durability of 3D-Printed Cementitious Materials for Potential Applications in Structures Exposed to Marine Environments

Fabian B. Rodriguez[1](✉), Cristian Garzon Lopez[3], Yu Wang[1], Jan Olek[1], Pablo D. Zavattieri[1], Jeffrey P. Youngblood[2], Gabriel Falzone[4], and Jason Cotrell[4]

[1] Lyles School of Civil Engineering, Purdue University, West Lafayette, IN, USA
rodri563@purdue.edu
[2] School of Materials Engineering, Purdue University, West Lafayette, IN, USA
[3] Facultad de Ingeniería, Universidad Nacional de Colombia, Bogotá, Colombia
[4] RCAM Technologies, Los Angeles, CA, USA

Abstract. The rising interest in 3D-printing of concrete structures for use in marine environments requires development of concrete mixtures with adequate mechanical and durability characteristics. The incorporation of alternative cementitious materials, combined with careful selection of printing parameters has emerged as an effective way of controlling not only the fresh properties and printability of mixtures, but also their mechanical and durability properties. This paper presents the results of various durability related tests performed on 3D-printed mortars, including density, porosity, rate of water absorption and resistance to chloride penetration. Results of these tests indicate that the performance of mortar elements 3D-printed using controlled overlap process was similar to the performance of conventionally cast mortar elements with the same composition. Moreover, the results of the chloride transport related tests obtained from all specimens evaluated during the course of the study indicate low chloride ion penetrability, thus re-affirming that combination of the proposed material and 3D-printing method of fabrication have a potential for producing structural elements for applications in marine environments.

Keywords: 3D-printed concrete · Durability · Corrosion · Chlorides · Absorption

1 Introduction

3D-Concrete Printing (3DCP) process has been intensively explored for a variety of construction applications [1]. Early efforts focused on the development of 3D-printing systems and mixtures designs with suitable rheological and mechanical properties [2]. More recent efforts focus on 3D-printing of structures containing reinforcement and on evaluation of their mechanical and durability characteristics [3]. In addition, the increased global interest in renewable energy generation has accelerated the development

R. Buswell et al. (Eds.): DC 2022, RILEM Bookseries 37, pp. 175–181, 2022.
https://doi.org/10.1007/978-3-031-06116-5_26

of offshore wind energy projects. These projects represent an excellent opportunity for the use of 3DCP for manufacturing wind turbine towers, anchors, and foundations for offshore projects [4]. In these applications, the design and manufacture of 3D-printed structures must account for factors related to durability of concrete exposed to chlorides, sulfates, and magnesium ions. Appropriate testing methods are also required to estimate the durability performance of 3DCP materials [5].

The role of 3D-printing process-induces heterogeneities within the manufactured elements, such as cold joints, macropores and interfacial regions, along with parameters that control these heterogeneities, have already been extensively studied in the past [6, 7]. However, the study of their effects on the transport properties of chlorides and the susceptibility to corrosion has been limited.

This paper presents the results of evaluation of selected durability characteristics of cementitious mixtures developed for potential applications in 3D-printed structures exposed to marine environment. The internal structure of elements produced a gantry-style and robotic arm, was modified by adjusting the printing parameters that control the geometry of individual filaments to create an overlap of the adjoining filaments. Specifically, the influence of the degree of filament overlap on the absorption and transport characteristics of 3D-printed elements was investigated.

2 Materials and Methods

The materials used in the fabrication of cast and 3D-printed specimens included the following: Type I ordinary portland cement (OPC) compliant with ASTM C150, limestone filler, silica fume, Class C fly ash compliant with ASTM C618, sand with a maximum particle size of 4.75 mm, polycarboxylate-based high range water-reducing admixture (HRWRA) meeting the requirements of ASTM C494 for type F admixtures, viscosity-modifying admixture (VMA) meeting the requirements of ASTM C494 for type S admixtures and tap water. An additional mixture, M13+CC, used for evaluation of rapid chloride penetration and water absorption, included calcined clay as the supplementary cementitious material (SCM) and rheology modifying material. The proportions of the two types mixtures used in the study are given in Table 1.

Table 1. Mixture proportioning of 3DCP.

Name	Cementitious materials (kg/m^3)					Admixtures (mL/100 kg)	
	Cement	Fly Ash class C	Silica fume	Limestone filler	Calcined Clay	HRWRA	VMA
M13	377.6	125.9	62.9	62.9	–	468	1192
M13+CC	377.6	125.9	62.9	62.9	31.5–	468	1192

The 3D-printed elements used in the study were produced using two types of printers: (a) the Hyrel Hydra 16A printer (0.6 m by 0.35 m by 0.2 m building size) with a 16 mm

nozzle opening (Fig. 1a), and (b) the ABB 6-axis robotic arm (2.65 m maximum reach) with a 25 mm nozzle opening (Fig. 1b). The filament height was set to 10 mm for the different printing configurations and the nominal filament width for the toolpath was set between 20 and 30 mm. However, the actual printed filament width (i.e., estimated extruded width based on the printing parameters) varied from 25 to 40 mm (Fig. 1c–1f). The printing parameters used for the different elements are presented in Table 2. The filament overlap percentage, defined as the difference between the printed width of the filament and the nominal filament width expressed as a percentage of the latter (Fig. 1f), was varied by altering the pump flow rate. The effect of overlap percentage on durability was subsequently evaluated.

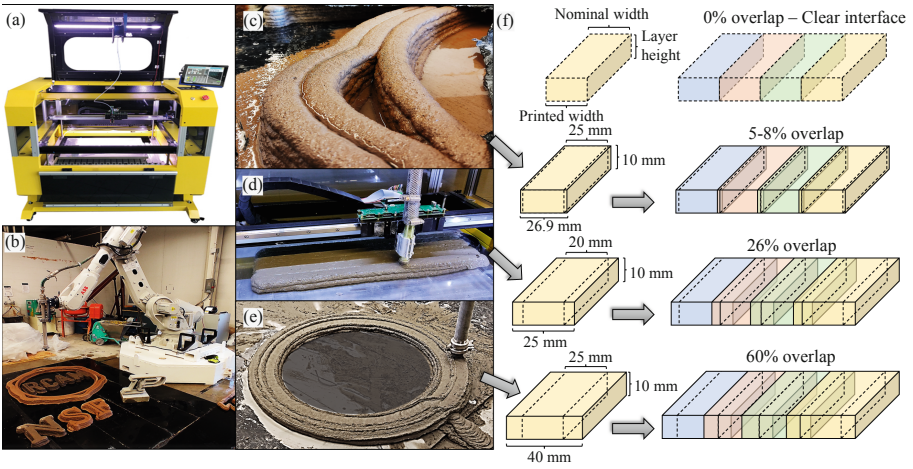

Fig. 1. a) Hyrel-16A printer; b) 6-axis robotic arm; c–e) 3DCP elements produced with different filament overlap values; f) Dimensions of filaments and overlap of the 3D-printed layers.

Table 2. Printing parameters used in 3DCP process.

Printer	Material	Nozzle size	Printing speed	Nominal width	Estimated width	Overlap
		(mm)	(mm/s)	(mm)	(mm)	(%)
Hyrel	M13	16	50	25	26.9	8
Hyrel	M13	16	100	20	25.2	26
Robot Arm	M13	25	200	25	40.3	61
Robot Arm	M13+CC	25	150	30	31.4	5

Different types of durability-related tests were performed on specimens obtained from 100 mm diameter cast cylinders and cores extracted from 3D-printed prismatic elements. In general, the test procedures followed the relevant ASTM standards with small modifications as described in the next paragraph. All specimens were tested after

60 days of curing with the exception of samples from M13+CC mixture which were cored at 28 days. The tests performed are summarized as follows:

The densities, absorptions and volumes of permeable voids were determined following the procedure given in ASTM C642 except that the vacuum saturation, rather than water boiling, was used for purposes of determination of internal porosity of the specimens. The water-absorption tests followed ASTM C1585, except that the specimens were dried at 60 ºC, rather than at 50 ºC following the procedure described by Zhutovsky and Hooton [8]. This process has been demonstrated to improve the uniformity of sorptivity measurements and provide data which correlate better with other transport properties. Indication of chloride ions penetration was evaluated by conducting electrical conductance tests following the ASTM- C1202 standard. The total charged passed was adjusted considering the nominal cross-sectional areas of the cylinder.

3 Experimental Results

An initial assessment of the quality of the internal structure of 3D-printed elements was made through the determination of the bulk and apparent densities. Figure 2a shows that the measured densities values for different configurations of 3D-printed elements are comparable to the cast specimens. This suggests that the 3D-printing process which involves overlap of the filaments does not lead to the reduction in density commonly observed in 3DCP materials. Moreover, the results for the percentage of permeable pore space and absorption levels of 3D-printed specimens (Fig. 2b), indicate minor reduction with an increase in filament overlaps (2%–4% and 1%–2% respectively), possibly caused by the elimination of vertical interfaces. This hypothesis was evaluated further using the results of rate of absorption and chloride penetration tests.

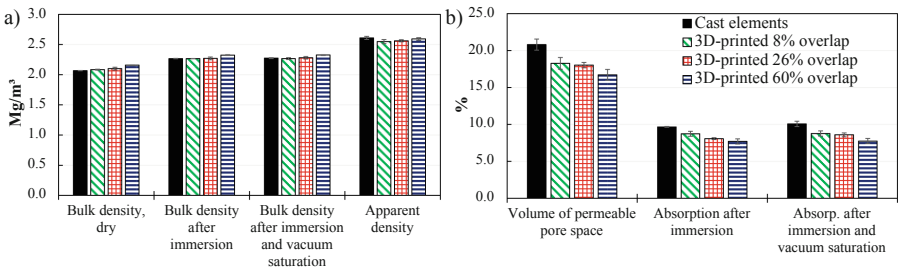

Fig. 2. a) Bulk densities and apparent density; b) Volume of permeable pore space an absorption, for cast elements and different types of 3D-printed elements.

The results of water absorption tests are presented on Fig. 3a–3c. Initial and secondary rates of absorption were determined based on a linear relationship between the absorption (I) and the square root of time ($s^{1/2}$) with a correlation coefficient of at least 98%. Of the five types of specimens tested, the 3D-printed specimens from mixture M13+CC with 5% overlap and M13 with 8% overlap resulted, respectively, in the highest and second highest of both, the initial and the secondary rates of absorption. In contrast, mixture

M13 with 26% and 60% overlap exhibited rates of absorption similar to those of cast specimens. However, the variability of the results for specimens with 60% overlap was higher compared to that observed for cast and 3D-printed specimens with 26% overlap. This demonstrates that overlapping of adjacent filaments has a significant effect with respect to reducing the level of absorption of 3D-printed elements. However, it should be pointed out that extreme overlapping, such as 60%, did not result in significant additional improvement in the permeability values.

The results of the rapid chloride penetration tests performed on the five sets of specimens are shown in Fig. 3d. These results also show a significant effect of filaments overlap on the total electrical charge passed. According to ASTM C1202, a very low potential for chloride ions penetrability is estimated for charge values between 100 and 1000 coulombs. It can be seen that three of the five types of specimens (i.e., cast and 3D-printed with 26% and 60% overlap) fall into this category. In contrast, 3D-printed elements with 5% and 8% overlap fall within the "low penetrability" category.

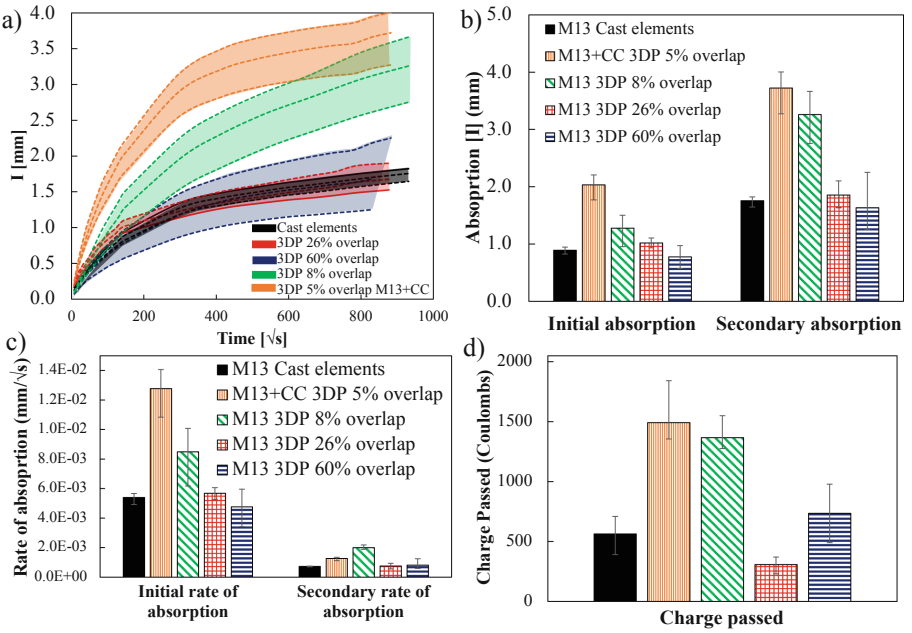

Fig. 3. (a) Results of a)water absorption showing the range of results and average absorption values (dotted lines); b) Initial and secondary absorption; c) Initial and secondary rates of absorption; d) Rapid chloride penetration test, for cast and 3D-printed specimens.

4 Discussion

Based on the previous results, it is possible to identify the beneficial effect of adjusting the printing parameters to produce an overlap of the filaments with respect to the

designed toolpath. The data suggests that a significant improvement in the quality of the microstructure of 3D-printed elements was achieved when transitioning from an 8% to a 26% overlap. This was achieved by extruding material over a segment of previously deposited filament in order to "densify" the interfacial regions, which are typically more susceptible to development of higher porosity. At 5% and 8% overlap it is surmised that the material from freshly extruded filament does not merge with the existing filament creating a weak bond influenced by the speed of the nozzle and gravity acting on the filament. For intermediate overlap, such as 26%, results of absorption and chloride transport suggest that the internal structure of the elements, specially, the quality of the interfacial region is improved by fusing the extruded filament with the existing one, without affecting the stability of the layer. However, it is evident that an excessive overlap can have detrimental effects to the structure of the elements. Elements with 60% overlap show higher values of conductance, as well as higher variability in the capillary pore system. In this case, it is surmised that increasing flow of material extruded around the interfacial region of the filaments may cause the lateral displacement of the material in the previously deposited filament and subsequent creation of discontinuities and high-porosity regions, affecting the quality of the printed layer and the whole element. At present, only limited number of studies focused on quantitative evaluation of absorption and chloride penetration levels on 3D-printed elements [9]. Thus, comparisons are often made with studies conducted on cast concrete. However, significant differences in composition of mixtures used for 3D printing and those used for traditional, i.e., cast concretes pose a difficulty with respect to evaluating the effects of 3D-printing on durability of resulting elements.

5 Conclusions

The current work demonstrated that the controlled overlap of the adjacent 3D-printed concrete filaments influenced the transport properties of resulting elements. 3D printed elements with a moderate level of filament overlap attained durability performance comparable to cast counterparts. This approach is useful for 3D-printing applications that require reduced permeability to avoid durability problems (e.g., reinforcement corrosion). Further exploration of the effects of the percentage of overlap, interlayer permeability and its interdependence on material's rheology and printing time intervals is required to proof the efficacy of this approach in more general conditions.

References

1. Grasser, G., Pammer, L., Köll, H., Werner, E., Bos, F.P.: Complex architecture in printed concrete: the case of the Innsbruck University 350th Anniversary Pavilion COHESION. In: Bos, F.P., et al. (eds.): DC 2020, RILEM Bookseries, vol. 28, pp. 1116–1127 (2020). https://doi.org/10.1007/978-3-030-49916-7_106
2. Blaakmeer, J., Lobo, B.: A robust mortar and printing system. In: Bos, F.P., et al. (eds.) DC 2020, RILEM Bookseries, vol. 28, pp. 1091–1103 (2020). https://doi.org/10.1007/978-3-030-49916-7_104

3. Bos, F.P., Ahmed, Z.Y., Wolfs, R.J.M., Salet, T.A.M.: 3D printing concrete with reinforcement. In: Hordijk, D.A., Luković, M. (eds.) High Tech Concrete: Where Technology and Engineering Meet, pp. 2484–2493. Springer, Cham (2018). https://doi.org/10.1007/978-3-319-59471-2_283
4. Wu, Y.C., Cotrell, J., Li, M.: Interlayer effect on fracture behavior of 3D printing concrete. In: Bos, F.P., et al. (eds.) DC 2020, RILEM Bookseries, vol. 28, pp. 537–546 (2020). https://doi.org/10.1007/978-3-030-49916-7_55
5. Rehman, A.U., Kim, J.H.: 3D concrete printing: a systematic review of rheology, mix designs, mechanical, microstructural, and durability characteristics. Materials **14** (2021)
6. Moini, M., Olek, J., Magee, B., Zavattieri, P.D., Youngblood, J.P.: Additive manufacturing and characterization of architectured cement-based materials via X-ray micro-computed tomography. In: Wangler, T., Flatt, R.J. (eds.) DC 2018, RILEM Bookseries, vol. 19, pp. 176–189 (2019). https://doi.org/10.1007/978-3-319-99519-9_16
7. Wolfs, R.J.M., Bos, F.P., van Strien, E.C.F., Salet, T.A.M.: A real-time height measurement and feedback system for 3D concrete printing. In: Hordijk, D.A., Luković, M. (eds.) High Tech Concrete: Where Technology and Engineering Meet, pp. 2474–2483 (2017). https://doi.org/10.1007/978-3-319-59471-2_282
8. Zhutovsky, S., Douglas Hooton, R.: Role of sample conditioning in water absorption tests. Constr. Build. Mater. **215**, 918–924 (2019)
9. Van Der Putten, J., De Volder, M., Van den Heede, P., De Schutter, G., Van Tittelboom, K.: 3D printing of concrete: the influence on chloride penetration. In: Bos, F.P., et al. (eds.) DC 2020, RILEM Bookseries, vol. 28, pp. 500–507 (2020). https://doi.org/10.1007/978-3-030-49916-7_51